

Signatures of a quantum phase transition on a single-mode bosonic model

Emmanouil Grigoriou¹ and Carlos Navarrete-Benlloch^{1,2,*}

¹*Wilczek Quantum Center, School of Physics and Astronomy,
Shanghai Jiao Tong University, Shanghai 200240, China*

²*Shanghai Research Center for Quantum Sciences, Shanghai 201315, China*

Equilibrium phase transitions usually emerge from the microscopic behavior of many-body systems and are associated to interesting phenomena such as the generation of long-range order and spontaneous symmetry breaking. They can be defined through the non-analytic behavior of thermodynamic potentials in the thermodynamic limit. This limit is obtained when the number of available configurations of the system approaches infinity, which is conventionally associated to spatially-extended systems formed by an infinite number of degrees of freedom (infinite number of particles or modes). Taking previous ideas to the extreme, we argue that such a limit can be defined even in non-extended systems, providing a specific example in the simplest form of a single-mode bosonic Hamiltonian. In contrast to previous non-extended models, the simplicity of our model allows us to find approximate analytical expressions that can be confronted with precise numerical simulations in all the parameter space, particularly as close to the thermodynamic limit as we want. We are thus able to show that the system undergoes a change displaying all the characteristics of a second-order phase transition as a function of a control parameter. We derive critical exponents and scaling laws revealing the universality class of the model, which coincide with that of more elaborate non-extended models such as the quantum Rabi or Lipkin-Meshkov-Glick models. Analyzing our model, we are also able to offer insights into the features of this type of phase transitions, by showing that the thermodynamic and classical limits coincide. In other words, quantum fluctuations must be tamed in order for the system to undergo a true phase transition.

I. INTRODUCTION

Depending on the environmental conditions, systems may exhibit strikingly different behaviors. To account for these differences, the concept of ‘phase’ is often employed [1]. They may be familiar equilibrium phases such as solid or liquid, but also more exotic such as dynamical [2] or topological [3]. As one parameter is varied, the system can change phase through a crossover or by undergoing a phase transition. In the presence of the latter, the boundary between phases can be defined through a critical point, around which the system will exhibit characteristic phenomena such as the divergence of the correlation length and the slow down of the dynamics, which are notorious hurdles to simulations. These phenomena, often dubbed critical phenomena, come with some subtleties that are still a subject of research. For example, the generation of long-range order and the corresponding divergence of the correlation length are still considered fundamental components of criticality, although recent works [4, 5] have hinted at the presence of phase transitions in spatially non-extended systems.

An interesting feature of phase transitions is the fact that similar critical behavior is observed across a broad spectrum of models coming from seemingly unrelated topics in physics, chemistry, and even biology. In the case of equilibrium continuous phase transitions, these connections are now understood through the well-established concept of universality [6–8] and the emergent nature

of the macroscopic properties characterizing the equilibrium phases. This results in the possibility of gathering critical behavior in universality classes, characterized by how the emergent properties behave around the critical point as the thermodynamic limit is approached. As a natural consequence, in order to disentangle the essential physics relevant to criticality from other intricate phenomena or to test new theoretical and numerical tools, finding the simplest model within a particular universality class is a very relevant task.

This point is well illustrated within the realm of equilibrium quantum phase transitions. Conceptually, these are a consequence of abrupt changes in the ground state of the system as we smoothly vary a parameter of its underlying Hamiltonian. The phase change is not driven by thermal fluctuations and can occur even at zero temperature [9]. Consequently, it is sometimes said that the phase change is driven by quantum fluctuations. Experimentally accessible imprints commonly survive finite temperatures as indicated by, e.g., the superconducting-insulator transition [10] or the transverse-field Ising model [11]. In this respect, the last decades have seen a flourishing number of technological platforms leading the field of many-body physics to an ever increasing number of experimental observations, in particular within the scope of condensed-matter systems. In order to meet modern technological needs, materials with complex electronic structures displaying conductor-insulator transitions, heavy fermion compounds, and two-dimensional electron gases [12] have become topics of vivid interest. Many conceptual mysteries remain within such complex systems, with predictions heavily relying on costly numerical methods [13] and quantum simulating platforms

* corresponding author; derekkorg@gmail.com

such as optical lattices [14–17]. This complexity has highlighted the necessity for new theoretical ideas and novel approaches, driving the community towards simpler platforms. For instance, engineering of quantum phase transitions in artificial nanoscale devices such as quantum dots [18, 19] is one of such attempts.

Central to the mathematical framework of phase transitions lies the concept of thermodynamic limit. This limit is obtained when the number of available configurations of the system approaches infinity, which traditionally has been associated with a divergent number of system constituents [6, 9], in turn usually linked to the physical extension of the system approaching infinity. This is indeed the case of the paradigmatic transverse-field Ising model [20], for example, where the thermodynamic limit is obtained when the size of the lattice that hosts one spin at each node diverges. Recently, however, the intriguing possibility of using the infinite-dimensional Hilbert space of a single harmonic oscillator (which in principle already provides an infinite number of available configurations), has motivated researchers to study non-extended systems such as the Dicke [21], quantum Rabi [5], or Jaynes-Cummings [4] models. All of these consist of a single bosonic mode coupled to a finite spin. It is argued that its ground-state energy possesses a critical point as a function of the coupling strength, with the thermodynamic limit determined by the ratio between the characteristic energy scales of the bosonic mode and the spin. Moreover, for the first two models, the phase transition is found to be in the same universality class as previously known mean-field models such as the Lipkin-Meshkov-Glick (LMG) model [22, 23], where an infinite number of two-level systems interact all with one another, which can be equivalently formulated as a model for a single large spin.

In this work, we further argue that phase transitions can be defined in systems that are not spatially extended, by going to the extreme of developing a model containing only a single bosonic mode. According to conventional definitions, the system undergoes a change as a function of a control parameter that displays all the characteristics of a second-order phase transition. In particular, to our knowledge, we provide here the simplest model within the same universality class as the quantum Rabi and LMG models. The simplicity of the model allows us to characterize it from first principles in all the parameter space, giving solid support to the various analytical approximations that we use to get physical insight. Furthermore, our model allows us to prove an interesting point: the thermodynamic limit in which the critical behavior appears scales with the number of excitations and is shown to coincide with the classical limit in which quantum fluctuations become negligible. The simplicity of our model also makes it a perfect one as a building block for more complex lattice structures that might present interesting interplays between many-body and local critical phenomena.

Let us outline the contents of this article. In Section II

we introduce the model, its approximate ground states, and the numerical approach that allows us to study it in all parameter space. In Section III we present our main results, studying the behavior of the system around the critical point and determining that it offers all the signatures of a second-order phase transition. In Section IV we discuss the sensitivity of the model to symmetry-breaking perturbations when in the ordered phase, and in Section V we conclude and discuss some subtleties related to the equivalence between the thermodynamic and classical limits.

II. MODEL AND METHOD

Consider the single-mode bosonic Hamiltonian

$$\hat{H} = \hat{a}^\dagger \hat{a} - \frac{\varepsilon}{2} (\hat{a}^{\dagger 2} + \hat{a}^2) + \frac{1}{2L} \hat{a}^{\dagger 2} \hat{a}^2, \quad (1)$$

where \hat{a}^\dagger and \hat{a} are creation and annihilation operators satisfying the canonical commutation relation $[\hat{a}, \hat{a}^\dagger] = 1$. Note that we have normalized the energy scale to the parameter of the first term, which depending on the implementation has different physical significance (e.g., the detuning with respect to a driving field in quantum optics [24] or a chemical potential in an atomic gas [14–17]). The parameter $\varepsilon > 0$ breaks particle-number conservation and is associated with the coherent injection of pairs of bosons, while the parameter $1/L > 0$ is associated to the nonlinearity or repulsive interactions between the bosons. We will see that ε is responsible for crossing a phase transition, while L controls how close we are to the thermodynamic limit. Note that this Hamiltonian has a discrete Z_2 symmetry, as it is invariant under the parity transformation $\hat{U} = e^{i\pi \hat{a}^\dagger \hat{a}}$, which acts as $\hat{U}^\dagger \hat{a} \hat{U} = -\hat{a}$.

One motivation to study this model is that, in contrast to the previous ones, we find ways to analyze it in all the region of the parameter space (ε, L) both through approximate analytical techniques and first-principles numerical ones. In the reminder of this section we explain the different approaches that we use: Coherent-state (classical) ansatz, Bogoliubov-de Gennes theory around the classical minima, general Gaussian ansatz, and full numerical simulations via a well-chosen basis of the Hilbert space. These methods will univocally show that there is a second-order phase transition at $\varepsilon = 1$ for $L \rightarrow \infty$ that belongs to the same universality class as the phase transition present in the quantum Rabi and LMG models.

Let us first explore the classical limit of this model. We make a coherent-state ansatz $|\alpha\rangle$ [24], characterized by being a right (left) eigenstate of the annihilation (creation) operators, i.e. $\hat{a}|\alpha\rangle = \alpha|\alpha\rangle$. The corresponding classical energy function is

$$E(\alpha, \alpha^*) = \langle \alpha | \hat{H} | \alpha \rangle = \frac{|\alpha|^4}{2L} + |\alpha|^2 - \frac{\varepsilon}{2} (\alpha^{*2} + \alpha^2). \quad (2)$$

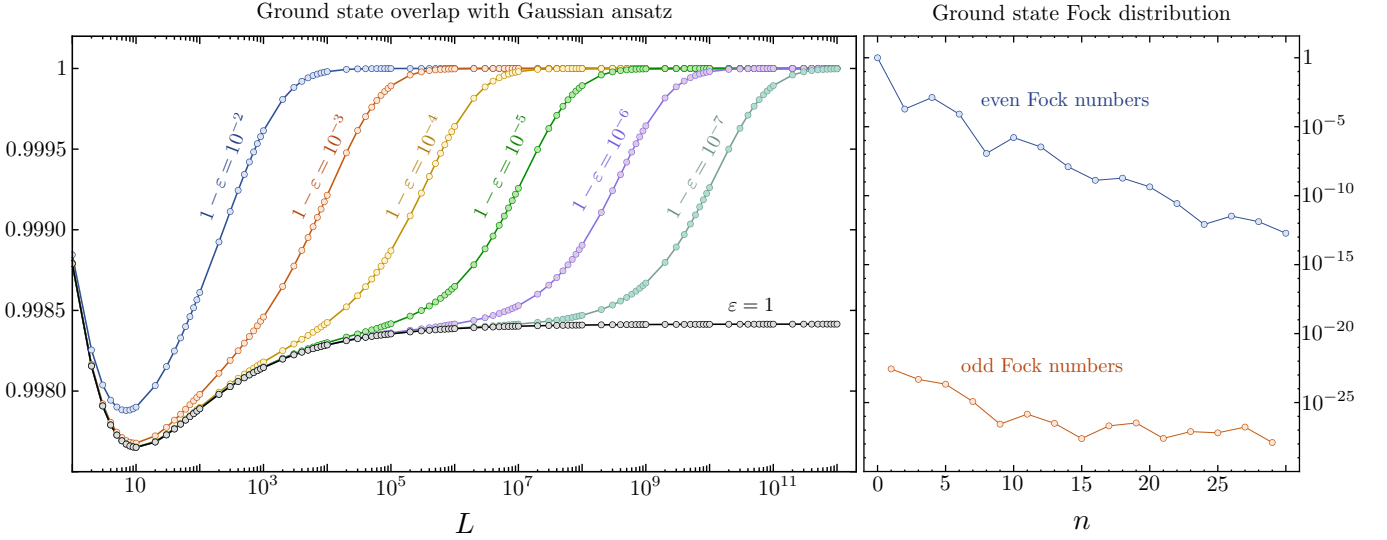


Figure 1. (Left panel) Overlap $|\langle 0|\hat{S}^\dagger(\bar{z})|\psi_{\text{GS}}\rangle|^2$ between the true ground state $|\psi_{\text{GS}}\rangle$ of the system and the Gaussian ansatz $\hat{S}(\bar{z})|0\rangle$ as a function of the system size L for different values of the pair injection rate ε close to the critical point $\varepsilon = 1$. (Right panel) Fock distribution $|\langle n|\hat{S}^\dagger(\bar{z})|\psi_{\text{GS}}\rangle|^2$ of the true ground state of the system for $L = 10^{12}$ at the critical point.

Since the first two terms are positive and depend only on the magnitude of α , the energy is obviously minimized for $\alpha \in \mathbb{R}$, since then the last term is the smallest possible for any given magnitude $|\alpha|$. The classical energy takes the simple form

$$E(\alpha) = (1 - \varepsilon)\alpha^2 + \frac{1}{2L}\alpha^4, \quad (3)$$

which changes from a single-well structure for $\varepsilon \leq 1$ with minimum at $\alpha = 0$, to a double-well one for $\varepsilon > 1$ with minima at $\alpha = \pm\sqrt{L(\varepsilon - 1)}$. In other words, the trivial state $\alpha = 0$ becomes unstable for $\varepsilon > 1$ in favor of two non-trivial states each of which break the Z_2 symmetry. As we will see later, quantum mechanically it is shown that there is indeed a second-order phase transition. This simple classical picture lays the intuition of the system.

In order to go further quantum mechanically, but still allowing for some analytics, we consider small quantum fluctuations around the classical minima α . To this aim, we move to a picture displaced to the corresponding phase-space location, defined by the unitary transformation operator $\hat{D}(\alpha) = \exp(\alpha\hat{a}^\dagger - \alpha^*\hat{a})$, the so-called displacement operator. Any state $|\psi\rangle$ is transformed into $\hat{D}^\dagger(\alpha)|\psi\rangle$, which evolves according to the Hamiltonian $\hat{h} = \hat{D}^\dagger(\alpha)\hat{H}\hat{D}(\alpha)$. Using $\hat{D}^\dagger(\alpha)\hat{a}\hat{D}(\alpha) = \hat{a} + \alpha$ and truncating to second order in creation and annihilation operators (which in this picture correspond to fluctuations around α) reads

$$\hat{h} \approx E(\alpha) + \Delta(\alpha)\hat{a}^\dagger\hat{a} - \frac{\sigma(\alpha)}{2}(\hat{a}^2 + \hat{a}^{\dagger 2}), \quad (4)$$

with

$$\Delta(\alpha) = 1 + \frac{2\alpha^2}{L}, \quad (5a)$$

$$\sigma(\alpha) = \varepsilon - \frac{\alpha^2}{L}. \quad (5b)$$

The linear term vanishes because the corresponding coefficient is equal to $\partial E/\partial\alpha$, which vanishes at the classical minima. We expect higher-order corrections to vanish in the $L \rightarrow \infty$ limit, as we indeed show when discussing Fig. 1 and the Gaussian ansatz below. Note that the eigenstates of \hat{h} are independent of L , since expressions (5) are independent of L at any of the classical minima α . Therefore, the ground state coming from this approximation can only be exact in the limit $L \rightarrow \infty$, which we identify later with the thermodynamic limit. Below we discuss how to approach the finite- L case.

Being quadratic, this approximate Hamiltonian \hat{h} is easily diagonalized via a Bogoliubov transformation, that is, in terms of a squeezed annihilation operator [24] $\hat{c} = \hat{S}(r)\hat{a}\hat{S}^\dagger(r) = \hat{a}\cosh r - \hat{a}^\dagger\sinh r$, with $\hat{S}(z) = \exp[(z\hat{a}^{\dagger 2} - z^*\hat{a}^2)/2]$, so that (4) takes the form

$$\hat{h} \approx E_0(\alpha) + \Omega(\alpha)\hat{c}^\dagger\hat{c}, \quad (6)$$

with

$$\Omega = \sqrt{\Delta^2 - \sigma^2}, \quad (7a)$$

$$E_0 = (\Omega - \Delta)/2, \quad (7b)$$

$$\sinh 2r = \sigma/\Omega. \quad (7c)$$

Note that stable, lower-bounded Hamiltonians require $\sigma \geq 0$ and $\Delta > \sigma$, which will be our case around the classical minima. The ground state of this Hamiltonian is

then the vacuum state of the Bogoliubov mode \hat{c} , or, coming back to the original mode and picture, the displaced squeezed vacuum state $\hat{D}(\alpha)\hat{S}(r)|0\rangle$, with $\hat{a}|0\rangle = 0$, which has energy E_0 . Let us now particularize these expressions to the classical minima that we found above.

Consider first the $\varepsilon \leq 1$ region, for which $\alpha = 0$, so that $\Delta = 1$ and $\sigma = \varepsilon$, leading to $\Omega = \sqrt{1 - \varepsilon^2}$ and $\sinh 2r = \varepsilon/\Omega$. In this case the approximate ground state $\hat{S}(r)|0\rangle$ is unique and invariant under the Z_2 symmetry transformation. Ω provides the gap to the first excited state, and closes at the critical point $\varepsilon = 1$, where the squeezing tends to infinity ($r \rightarrow \infty$).

When $\varepsilon > 1$, two degenerate classical energy minima appear, $\alpha = \pm\sqrt{L(\varepsilon - 1)} \equiv \alpha_{\pm}$, so that around either one of them $\Delta = 2\varepsilon - 1$ and $\sigma = 1$, leading to $\Omega = \sqrt{4\varepsilon(\varepsilon - 1)}$ and $\sinh 2r = 1/\Omega$. The degenerate ground space is in this case approximately spanned by displaced squeezed vacua $\hat{D}(\alpha_{\pm})\hat{S}(r)|0\rangle$. Both these states breaks the Z_2 symmetry spontaneously. The ground-state energy can be written as $E_0 = 1/2 - \varepsilon + \sqrt{(\varepsilon - 1)\varepsilon} - L(\varepsilon - 1)^2/2$. Note that, once again, the squeezing diverges at the critical point.

The discussion above hints at the system possessing two phases, a symmetry-preserving (disordered) and a symmetry-breaking (ordered) phase, separated by the critical point $\varepsilon = 1$. Note that the fact that the squeezing, and hence the number of excitations $\langle \hat{a}^\dagger \hat{a} \rangle = \sinh^2 r$, diverges at that point is compatible with the mode exploring its underlying infinite-dimensional Hilbert space, as required for the existence of a phase transition (in fact, we will later prove that $\langle \hat{a}^\dagger \hat{a} \rangle \sim L^{1/3}$ at the critical point, so that indeed L controls how close we are to the thermodynamic limit in this single-mode problem). However, we emphasize that the Bogoliubov-de Gennes approach above does not depend on L , is only approximate, and it diverges at the critical point, making it hardly a proof that there exists a true phase transition at the critical point. We then explore the problem with more accurate techniques, including a better Gaussian ansatz and an approximation-free numerical approach. Remarkably, the latter works for any value of the parameters (ε, L) by choosing an appropriate basis of the Hilbert space as we explain now and detail in Appendices A and B.

The numerical approach consists in finding the best Gaussian-state [24] estimate $\hat{D}(\bar{\alpha})\hat{S}(\bar{z})|0\rangle$ for the ground state of the system, and then building an appropriate basis of the Hilbert space around it. The ground-state ansatz is found by minimizing the energy functional $\langle \hat{H} \rangle$ with respect to the complex parameters $\bar{\alpha}$ and \bar{z} . We provide the details of this minimization in Appendix A. Whenever $\bar{\alpha} = 0$, we use the orthonormal set $\{\hat{S}(\bar{z})|n\rangle\}_{n=0,1,\dots,n_{\max}}$ to represent and diagonalize the (sparse) Hamiltonian, where $|n\rangle$ are Fock eigenstates satisfying $\hat{a}^\dagger \hat{a}|n\rangle = n|n\rangle$, and n_{\max} is a suitable truncation. If $\bar{\alpha} \neq 0$ we then use a non-orthonormal set $\{\hat{D}(\pm\bar{\alpha})\hat{S}(\bar{z})|n\rangle\}_{n=0,1,\dots,n_{\max}}$, corresponding to basis vectors around the two degenerate minima. We explain

all the nuances related to the use of a non-orthonormal set in Appendix B. Here it suffices to remark that using this optimized basis, convergence is found for small values of n_{\max} (say well below 100) no matter the choice of ε and L . This is because for small L the number of excitations $\langle \hat{a}^\dagger \hat{a} \rangle$ is small as well, while for large L the true ground state becomes closer to the Gaussian state ansatz. In particular, we find that for large but finite L the non-Gaussian fluctuations have a non-negligible (but still small) impact only extremely close to the critical point $\varepsilon = 1$. Moreover, for any ε we can find a sufficiently large value of L for which the ground state becomes Gaussian for all practical purposes. We illustrate this in Fig. 1a, where we plot the overlap between the true ground state and the Gaussian approximation $\hat{S}(\bar{z})|0\rangle$ as a function of L for different values of ε close to the critical point. For any ε , the overlap is already very close to 1 for small L , but jumps all the way to 1 (within numerical precision) as soon as L is large enough. From the tendency of the plot, we infer that at the critical point $\varepsilon = 1$ the overlap is exactly 1 only in the thermodynamic limit $L \rightarrow \infty$. Nevertheless, in Fig. 1b we show that even for finite L the Gaussian ansatz $\hat{S}(\bar{z})|0\rangle$ contains almost all the population of the ground state, with the contribution to any other basis states $\hat{S}(\bar{z})|n\rangle$ decreasing exponentially with n .

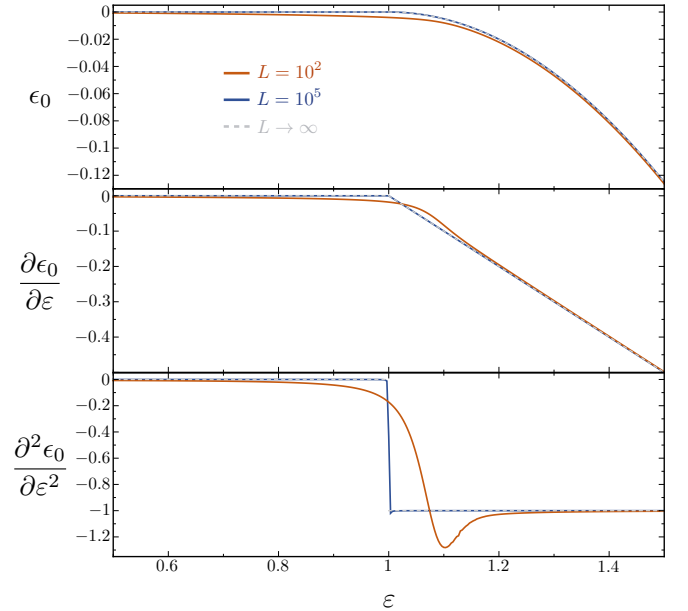


Figure 2. Ground-state energy density (and its derivatives) as a function of the pair injection rate ε . The grey-dashed line is the analytic prediction expected to be valid in the $L \rightarrow \infty$ limit, and predicting a discontinuity in the second order derivative (second-order phase transition). The orange and blue lines are numerical results for $L = 10^2$ and 10^5 , respectively, which indeed corroborate the expected analytical result.

III. MAIN RESULTS

A. Phase transition and critical exponents

We now present the results that characterize the phase transition. Let us start by discussing the ground-state energy density, which according to the approximate results presented above is predicted to be

$$\epsilon_0 = \lim_{L \rightarrow \infty} \frac{E_0}{L} = \begin{cases} 0 & \text{for } \varepsilon \leq 1 \\ -(\varepsilon - 1)^2/2 & \text{for } \varepsilon > 1 \end{cases} \quad (8)$$

Note first that this quantity is independent of L (making the energy extensive if L is interpreted as sort of a system-size parameter that controls how close we are to the thermodynamic limit, which we prove throughout the next sections). We represent this quantity, as well as its first and second order derivatives, as a function of ε in Fig. 2. Both ϵ_0 and its first derivative are continuous, while a discontinuity appears in the second derivative. This approximate expression then predicts a second-order phase transition in the thermodynamic limit. In the same figure we confront this prediction with the numerical results found for increasing values of L . The exact results approach the prediction of (8) as L increases.

In order to show that the phase transition belongs to the same universality class as the one of the quantum Rabi and LMG models, we first analyze the way in which observables behave when approaching the critical point. We consider here two observables, the gap between the two smallest Hamiltonian eigenvalues (counting degenerate ones as distinct), which we denote by ΔE , and the density of excitations $\rho = \langle \hat{a}^\dagger \hat{a} \rangle / L$. In Fig. 3 we show these quantities as a function of ε for increasing values of L (evaluated numerically), together with the asymptotic results predicted by the Bogoliubov approach of the previous section in the $L \rightarrow \infty$ limit:

$$\Delta E = \begin{cases} \sqrt{1 - \varepsilon^2} & \text{for } \varepsilon < 1 \\ 0 & \text{for } \varepsilon > 1 \end{cases}, \quad (9)$$

and

$$\rho = \begin{cases} 0 & \text{for } \varepsilon < 1 \\ \varepsilon - 1 & \text{for } \varepsilon > 1 \end{cases}. \quad (10)$$

The numerics confirm the Bogoliubov predictions. Moreover, given an observable quantity A , we expect it to be characterized around the critical point by a so-called critical exponent γ_A via a power law

$$\lim_{L \rightarrow \infty} A(\varepsilon, L) \propto |\varepsilon - 1|^{\gamma_A}. \quad (11)$$

The Bogoliubov theory developed above provides us with the exponents $\gamma_{\Delta E} = 1/2$ and $\gamma_\rho = 1$, the same exponents as those found in the quantum Rabi and LMG models [5]. For completeness, it is also interesting to look at the uncertainty of the position quadrature,

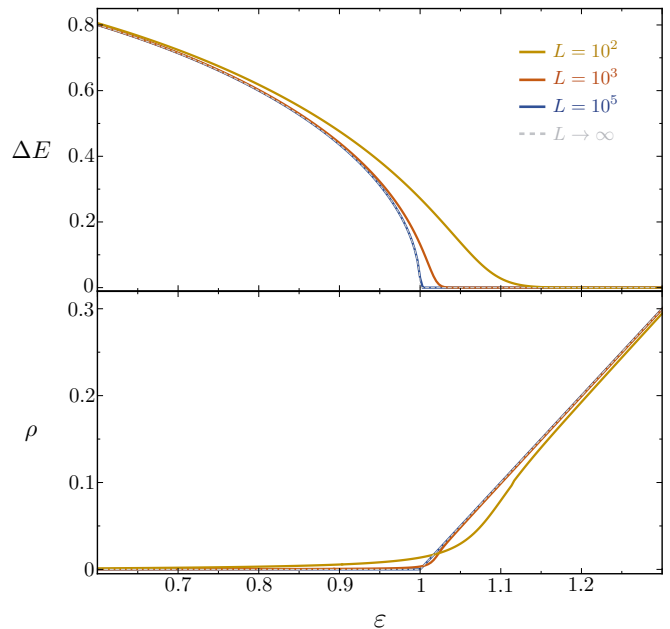


Figure 3. Energy difference ΔE between the two lowest eigen-energies (top) and density of excitations ρ (bottom) as a function of the pair injection rate ε . Similarly to the previous figure, the numerical results (solid lines) approach the expected analytical results (dashed lines) in the $L \rightarrow \infty$ limit.

$\hat{x} = \hat{a}^\dagger + \hat{a}$. For a pure Gaussian state $\hat{S}(r)|0\rangle$, this is just given by $\Delta x = e^r$. Noting that Bogoliubov-de-Gennes theory (below the critical point) predicts $\sinh 2r = \varepsilon / \sqrt{(1 + \varepsilon)(1 - \varepsilon)}$, so $e^{2r} \propto 1/\sqrt{1 - \varepsilon}$ around the critical point, we find $\gamma_{\Delta x} = -1/4$, exactly the one found in the quantum Rabi model as well [5].

B. Finite-size scaling and exponents

In order to confirm that our single-mode model is in the same universality class as the quantum Rabi and LMG models, we also need to analyze how criticality is approached as L increases. Here, we first consider the finite-size exponent δ_A associated to an observable A of interest, defined through:

$$\lim_{\varepsilon \rightarrow 1} A(\varepsilon, L) \propto L^{-\delta_A}. \quad (12)$$

In Fig. 4 we plot the same observables that we considered in the previous section, ΔE , ρ , and Δx , but now as a function of L for $\varepsilon = 1$. The numerical results show that they fit better and better a power-law of the type (12) as L increases. Bogoliubov theory is not useful to determine the finite-size exponents, since it has no information about L (implicitly assumes $L \rightarrow \infty$ as explained above). However, we can still estimate them by considering a squeezed-vacuum ansatz $\hat{S}(r)|0\rangle$, and minimizing the energy functional $\langle 0 | \hat{S}^\dagger(r) \hat{H} \hat{S}(r) | 0 \rangle$ at $\varepsilon = 1$. We show in Appendix A that this provides a scaling relation $e^{2r} \propto L^{1/3}$, with squeezing diverging as $L \rightarrow \infty$,

consistently with the Bogoliubov approach of the previous section. Using this ansatz, it is then easy to find the finite-size exponents $\delta_{\Delta E} = -1/3$, $\delta_\rho = -2/3$, and $\delta_{\Delta x} = 1/6$ (see Appendix A for details), which fit great the numerical results, as shown in Fig. 4. Remarkably, once again this scaling-law exponents coincide with those of the quantum Rabi and LMG models [5].

C. Scaling law

In order to prove beyond any doubt that the model displays a second-order phase transition and to completely determine its universality class, we need to prove that all physical observables A adhere to a scaling law of the type [7, 8]

$$A(\varepsilon, L) = C_1 |\varepsilon - 1|^{\gamma_A} F_A(C_2 |\varepsilon - 1|^\nu L), \quad (13)$$

around the critical point $\varepsilon = 1$ and the thermodynamic limit $L \rightarrow \infty$. The so-called correlation-length exponent ν must be the same for all observables, while the function F_A and the critical exponent γ_A depend on the observable. Models with the same scaling functions, critical exponents, and correlation-length exponents are said to belong to the same universality class. The coefficients C_j can differ between models and observables. In loose terms, the scaling law tells us that approaching the critical point either by varying the control parameter ε or the system's size L has the same effect, except for a well-defined scaling relation. Note that expressions (11) and (12) imply that the scaling function must satisfy

$$\lim_{y \rightarrow \infty} F_A(y) \propto 1, \quad (14a)$$

$$\lim_{y \rightarrow 0} F_A(y) \propto y^{-\frac{\gamma_A}{\nu}}. \quad (14b)$$

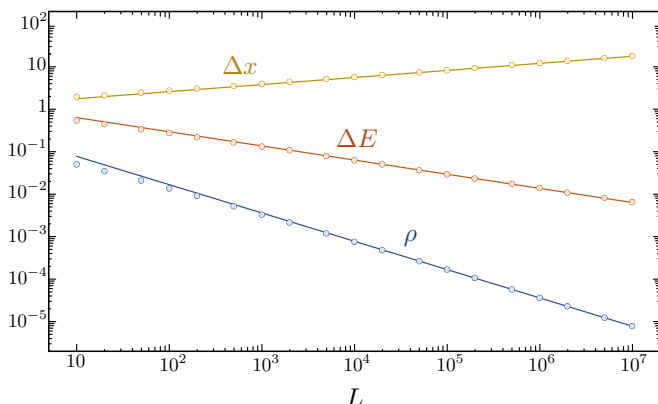


Figure 4. Log-log plot of the gap ΔE (red), density of excitations ρ (blue), and position uncertainty Δx (yellow) as a function of L at the critical point $\varepsilon = 1$. The circles are numerical results, while the solid lines are the linear expressions expected by the scalings found in the text. It is obvious that these match perfectly as L increases.

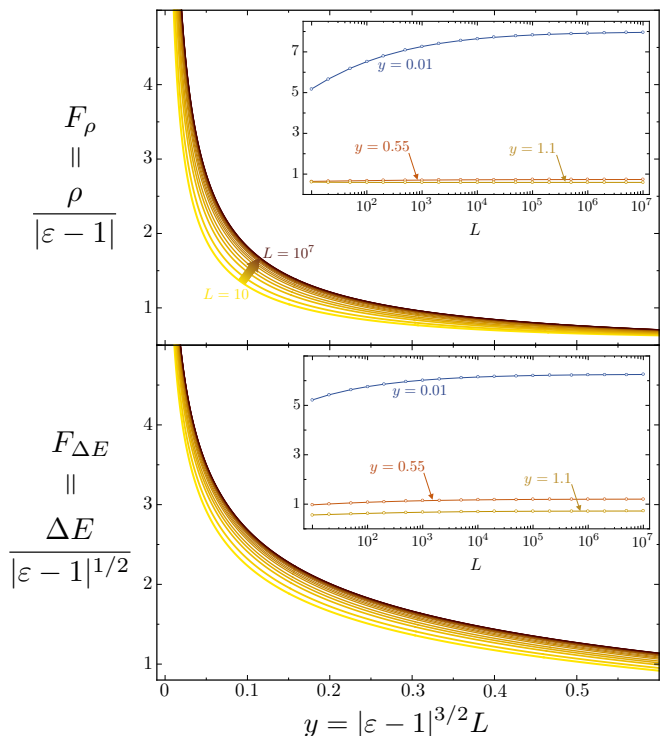


Figure 5. Scaling functions for the density of excitations ρ (top) and the gap ΔE (bottom). We can appreciate how the points obtained numerically converge to a well-defined curve as L increases (this is most clear in the insets, which show that the scaling functions saturate as a function of L for fixed y). We remark that we approach the critical point from below ($\varepsilon < 1$). However, we have checked that the same behavior appears when approaching it from above.

The second line provides a relation between the three characteristic exponents of the phase-transition, $\nu = \gamma_A / \delta_A$ for any observable A . For our model all three observables we have considered lead to the same correlation-length exponent, $\nu = 3/2$.

In Fig. 5 we show that our model satisfies a scaling law (13) by plotting $A(\varepsilon, L)|\varepsilon - 1|^{-\gamma_A}$ as a function of $y = |\varepsilon - 1|^\nu L$ for different values of ε and L , and two observables, the density of excitations ρ and the gap ΔE . As L goes towards infinity, all the points converge towards a well-defined curve $F_A(y)$, that satisfies the properties (14). Moreover, we have checked that the scaling function F_A is the same as the one of the quantum Rabi model (after matching the scaling coefficients C_j appropriately), and hence we conclude that they are indeed in the same universality class.

IV. SENSITIVITY TO SYMMETRY-BREAKING PERTURBATIONS

An interesting feature of systems undergoing phase transitions and spontaneous symmetry breaking is their sensitivity to infinitesimal external perturbations while

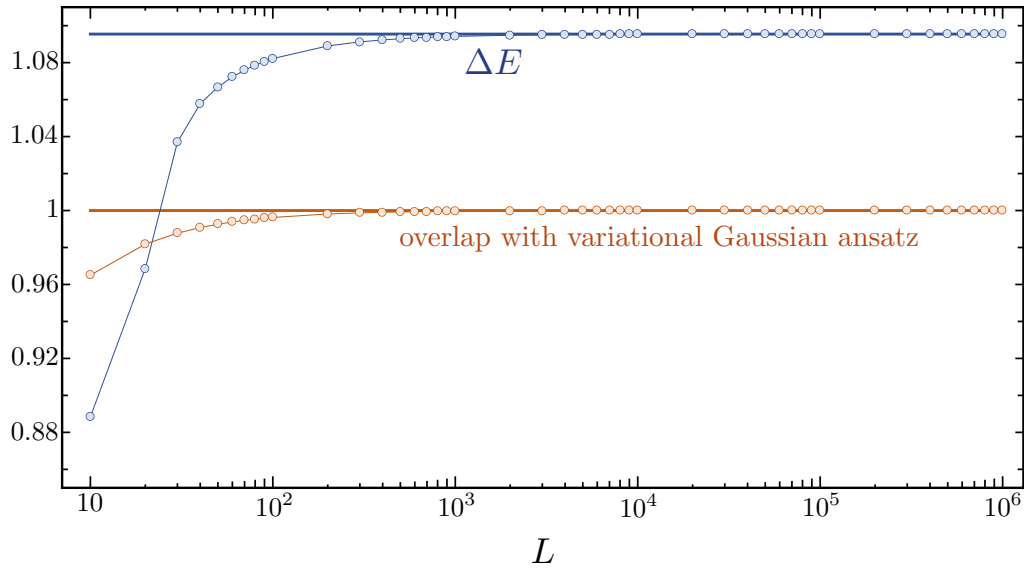


Figure 6. Gap between the two lowest energy eigenvalues (blue) and overlap of the ground state with a variational displaced squeezed vacuum state (red) as a function of L , when the Hamiltonian is perturbed by a symmetry-breaking term with coupling strength $\lambda = 1/\sqrt{L}$ for $\varepsilon = 1.3$. The circles are numerical results, while the solid lines are the results expected in the $L \rightarrow \infty$ limit.

in the ordered phase. In our case, for example, a finite gap should open in the ground-state manifold by adding a symmetry-breaking perturbation of the type

$$\hat{V} = \frac{i\lambda}{2} (\hat{a} - \hat{a}^\dagger), \quad (15)$$

to the Hamiltonian (1), with $\lambda \ll 1$. By numerically finding the two lowest-energy eigenstates, we show in Fig. 6 that, indeed, in the ordered region $\varepsilon > 1$ a perturbation $\lambda = 1/\sqrt{L}$ is enough to open a gap in the ground-state manifold of order larger than $\sqrt{\varepsilon - 1}$.

We gain analytical insight by making use of perturbation theory. Specifically, we consider the $L \rightarrow \infty$ limit, where the gap is closed for all practical purposes in the absence of perturbation, so that the ground-state manifold is two-dimensional, and approximately spanned by Gaussian states $\hat{D}(\pm\bar{\alpha})\hat{S}(\bar{z})|0\rangle$ (see Appendix A for details). In particular, the dominant contribution is expected to come from the displacement with $\bar{\alpha} = \sqrt{L(\varepsilon - 1)}$, so that in the following we approximate these states by coherent states $|\pm\bar{\alpha}\rangle$. Furthermore, in this $L \rightarrow \infty$ regime these states can be considered orthogonal, so that $\langle -\alpha|\hat{V}|\alpha\rangle = 0$. The corrections to the ground-state-manifold energies are then provided by $\langle \pm\alpha|\hat{V}|\pm\alpha\rangle = \mp\lambda\alpha$ within degenerate perturbation theory [25], hence predicting the opening of a gap within the ground-state manifold given by

$$\Delta E = 2\lambda\alpha = \sqrt{4\lambda^2 L(\varepsilon - 1)}, \quad (16)$$

which is finite in the ordered phase ($\varepsilon > 1, L \rightarrow \infty$) even for an infinitesimal parameter $\lambda \sim 1/\sqrt{L}$.

In Fig. 6 we plot the gap found numerically for $\varepsilon = 1.3$ and $\lambda = 1/\sqrt{L}$, as a function of L . We see that for large

L the numerical results converge to expression (16). In the same figure, we also plot the overlap between the numerical ground state and the variational Gaussian one $\hat{D}(\bar{\alpha})\hat{S}(\bar{z})|0\rangle$ (see Appendix A for more details). We can appreciate that these converge for large L , and moreover, we have checked that the variational parameters converge to the ones that we found with Bogoliubov theory in Section II.

V. DISCUSSION AND CONCLUSIONS

In summary, we have observed all the signatures required from a second-order phase transition in a single-mode bosonic model. The phase transition has been shown to be in the same universality class as those of more complex non-extended models such as the quantum Rabi and LMG models, making it the simplest model within this universality class (to our knowledge). The simplicity of our model allows us to bring up a subtle discussion related to whether one should call “quantum” phase transition (meaning a phase transition in the equilibrium state of the system at zero temperature, with the phase change driven by quantum fluctuations) to the type found in non-extended systems. Let us elaborate on this. First, let us point out that, as evidenced by the results above and proven in more rigor in Appendix C for our model, in these systems the thermodynamic limit coincides with the classical limit, that is, with the limit in which quantum fluctuations are irrelevant. In contrast, in extended systems the thermodynamic limit is usually controlled by their size, and local quantum fluctuations are still present even in the infinite-size limit. In this

sense, the phase transition of non-extended systems is less rich, and perhaps one cannot even claim that it is robust against quantum fluctuations, as they play no role in the thermodynamic or classical limit. Nevertheless, it is our belief that such systems are still worth exploring, since the elements required for a phase transition are present on them, and being non-extended they can be used as building blocks of more complex many-body models where the local phase transition of each block competes with other types of phase transitions effected by many-body phenomena.

ACKNOWLEDGMENTS

We thank Myung-Joong Hwang, Xiangjun Xing, and Soonwon Choi for interesting discussions. CNB thanks Valentina Hopekin for help with Figure 1, and acknowledges sponsorship from the Yangyang Development Fund, as well as support from a Shanghai talent program and from the Shanghai Municipal Science and Technology Major Project (Grant No. 2019SHZDZX01).

Appendix A: Gaussian minimization and finite-size exponents

In this section we discuss the details of the Gaussian-state ansatz $\hat{D}(\bar{\alpha})\hat{S}(\bar{z})|0\rangle$ that minimizes the energy of the system for any value of L . This ansatz has been crucial to determine the finite-size exponents in Section III B, to check the sensitivity to symmetry-breaking perturbations in Section IV, as well as to build a Hilbert-space basis leading to efficient numerical simulations, as explained in Sections II and Appendix B below. The variational parameters $\bar{\alpha}$ and \bar{z} are complex in principle, although we have found that the energy is minimized when both are taken real with \bar{z} positive. In particular, the energy functional has the form

$$E(\bar{\alpha}, \bar{z}) = \langle \hat{a}^\dagger \hat{a} \rangle - \varepsilon \text{Re}\{\langle \hat{a}^2 \rangle\} + \frac{\langle \hat{a}^{\dagger 2} \hat{a}^2 \rangle}{2L}. \quad (\text{A1})$$

We can use the identity [24] $\hat{S}^\dagger(\bar{z})\hat{D}^\dagger(\bar{\alpha})\hat{a}\hat{D}(\bar{\alpha})\hat{S}(\bar{z}) = \bar{\alpha} + \hat{a} \cosh \bar{r} + e^{i\theta} \hat{a}^\dagger \sinh \bar{r}$, with polar decomposition $\bar{z} = \bar{r}e^{i\theta}$ for the squeezing parameter, together with the definition $\delta \hat{a} \equiv \hat{a} - \langle \hat{a} \rangle$, to write the following useful expressions: $\langle \hat{a} \rangle = \bar{\alpha}$, $\langle \delta \hat{a}^2 \rangle = e^{i\theta} s_{2\bar{r}}/2$, and $\langle \delta \hat{a}^\dagger \delta \hat{a} \rangle = s_{\bar{r}}^2$, where we use the short-hand notation $s_x = \sinh x$. We then obtain

$$\begin{aligned} \langle \hat{a}^\dagger \hat{a} \rangle &= |\bar{\alpha}|^2 + s_{\bar{r}}^2, \\ \langle \hat{a}^2 \rangle &= \bar{\alpha}^2 + e^{i\theta} s_{2\bar{r}}/2, \\ \langle \hat{a}^{\dagger 2} \hat{a}^2 \rangle &= |\bar{\alpha}|^4 + 4|\bar{\alpha}|^2 s_{\bar{r}}^2 + \frac{1}{4} s_{2\bar{r}}^2 + 2s_{\bar{r}}^4 + \text{Re}\{\bar{\alpha}^{*2} e^{i\theta} s_{2\bar{r}}\}, \end{aligned} \quad (\text{A2})$$

which lead to a relatively simple energy functional that is easily minimized numerically with respect to the variational parameters with the use of any mathematics software. Note that in the last equation we have used the

Gaussian moment theorem [24] to write $\langle \delta \hat{a}^{\dagger 2} \delta \hat{a}^2 \rangle = 2\langle \delta \hat{a}^\dagger \delta \hat{a} \rangle^2 + |\langle \delta \hat{a}^2 \rangle|^2$, removing odd moments of the fluctuation operators.

At the critical point $\varepsilon = 1$ and for sufficiently large L , we expect $\bar{\alpha} = 0$ (which we also confirm numerically). Under such circumstances, only the second term in (A1) depends on θ , and is clearly minimized for $\theta = 0$. The energy functional can be written as a function of $x = e^{2\bar{r}}$ (expected to be large for large L), reading

$$E = \frac{3x^2}{32L} - \frac{x}{4L} - \frac{1}{2} + \frac{5}{16L} + \frac{1}{4x} \left(2 - \frac{1}{L} \right) + \frac{3}{32Lx^2}. \quad (\text{A3})$$

The derivative with respect to x reads

$$\frac{dE}{dx} = \frac{3x}{16L} - \frac{1}{4L} - \frac{1}{4x^2} \left(2 - \frac{1}{L} \right) - \frac{3}{16Lx^3}, \quad (\text{A4})$$

so that writing the minimization condition as

$$4Lx^3 \frac{dE}{dx} = \underbrace{\frac{3x^4}{4} - x^3 - \frac{3}{4}}_{\approx 3x^4/4} - \underbrace{(2L-1)x}_{\approx 2L} = 0, \quad (\text{A5})$$

we obtain the scaling $x \sim L^{1/3}$ provided in Section III B. Note that in (A5) we have used $x \gg 1$ and $L \gg 1$, but we have not assumed any particular dependence of x with L .

Once we know the scaling of $e^{2\bar{r}}$, it is easy to find the scaling for any observable. In the case of the number of excitations $\langle \hat{a}^\dagger \hat{a} \rangle = s_{\bar{r}}^2 \approx e^{2\bar{r}}/4$ and the quadrature variance $\langle \hat{x}^2 \rangle = e^{2\bar{r}}$, both of them scale with $L^{1/3}$, leading to the scalings provided in Section III B for the density $\rho = \langle \hat{a}^\dagger \hat{a} \rangle / L$ and the uncertainty $\Delta x = \sqrt{\langle \hat{x}^2 \rangle}$.

In order to determine the scaling of the gap, we take the variational excited states $\hat{S}(\bar{r})|n\rangle$, for consistency with our variational ground state. Using $\hat{S}^\dagger(\bar{r})\hat{a}\hat{S}(\bar{r}) = \hat{a} \cosh \bar{r} + \hat{a}^\dagger \sinh \bar{r}$, $\hat{a}|n\rangle = \sqrt{n}|n-1\rangle$, working at the critical point $\varepsilon = 1$, and defining the variational energy spectrum $E_n = \langle n|\hat{S}^\dagger(\bar{r})\hat{H}\hat{S}(\bar{r})|n\rangle$, it is easy to show after some algebra that

$$E_1 - E_0 = \frac{4 \sinh^4 r + 2 \sinh^2 2r}{2L} + e^{-2\bar{r}} \sim L^{-1/3}. \quad (\text{A6})$$

Appendix B: numerical simulation

In order to perform numerical diagonalization of the Hamiltonian, it is crucial to choose an appropriate basis. Here we show how to do this by building a basis from the Gaussian ansatz described in the previous section. It is first convenient to rewrite the Hamiltonian in terms of the Bogoliubov operators $\hat{c} = \hat{S}(\bar{r})\hat{a}\hat{S}^\dagger(\bar{r})$. In particular, we simply use the relation $\hat{a} = \hat{c} \cosh r + \hat{c}^\dagger \sinh r$, which inserted in (1) leads to an expression for \hat{H} as fourth-order polynomial in \hat{c} and \hat{c}^\dagger .

Whenever the optimization provides $\bar{\alpha} = 0$, we take $\{|n\rangle_c = \hat{S}(\bar{r})|n\rangle\}_{n=0,1,\dots,n_{\max}}$ as an orthonormal basis,

noting that $|n\rangle_c$ are the Fock states associated to the Bogoliubov operators, that is ${}_c\langle m|\hat{c}|n\rangle_c = \sqrt{n}\delta_{m,n-1}$. This leads to a simple sparse-matrix representation of \hat{H} , whose eigenvector with smallest eigenvalue is efficiently found with any algebra software, even when n_{\max} takes on extremely large values. On the other hand, we have checked that for all our simulations convergence is obtained way before that truncation, typically well before $n_{\max} \approx 100$.

The situation is a bit more complex when $\bar{\alpha} \neq 0$. In such case, we take $\{\hat{D}(\pm\bar{\alpha})|n\rangle_c\}_{n=0,1,\dots,n_{\max}}$ as the basis for the representation, built up from states localized around the two possible Z_2 -symmetry-breaking ground states. The issue here is that states with opposite displacement are not orthogonal, and hence, the basis vectors are not linearly independent. In order to explain how we deal with this, let us define and sort the basis elements as $\{|\phi_l\rangle\}_{l=0,1,\dots,2n_{\max}+1}$, with even elements $|\phi_{2n}\rangle = \hat{D}(\bar{\alpha})|n\rangle_c$, and odd ones $|\phi_{2n+1}\rangle = \hat{D}(-\bar{\alpha})|n\rangle_c$, where $n = 0, 1, \dots, n_{\max}$. We define the overlap matrix \mathcal{A} with elements $\mathcal{A}_{kl} = \langle\phi_k|\phi_l\rangle \neq \delta_{kl}$. We can insert the expansion $|\psi\rangle = \sum_l y_l|\phi_l\rangle$ into the eigenvalue equation $\hat{H}|\psi\rangle = \lambda|\psi\rangle$, and apply $\langle\phi_k|$ onto it, obtaining the generalized eigenvalue problem

$$\mathcal{H}\mathbf{y} = \lambda\mathcal{A}\mathbf{y}, \quad (\text{B1})$$

where the representation \mathcal{H} of the Hamiltonian has components $\mathcal{H}_{kl} = \langle\phi_k|\hat{H}|\phi_l\rangle$ and $\mathbf{y} = (y_0, y_1, \dots, y_{2n_{\max}+1})^T$. While this is no longer a sparse problem, the ground state can be efficiently found with any algebra software as well, especially keeping in mind that convergence is found for $n_{\max} < 100$ once again. The only tricky point we want to emphasize is related to how to write the matrices \mathcal{A} and \mathcal{H} . In the case of the overlap matrix, we use

$$\mathcal{A}_{2q,2p} = \langle\phi_{2q}|\phi_{2p}\rangle = \langle q|\hat{D}^\dagger(\bar{\alpha})\hat{D}(\bar{\alpha})|p\rangle = \delta_{qp}, \quad (\text{B2})$$

$$\mathcal{A}_{2q,2p} = \langle\phi_{2q+1}|\phi_{2p+1}\rangle = \langle q|\hat{D}^\dagger(-\bar{\alpha})\hat{D}(-\bar{\alpha})|p\rangle = \delta_{qp},$$

$$\begin{aligned} \mathcal{A}_{2q+1,2p} &= \langle\phi_{2q+1}|\phi_{2p}\rangle = \langle q|\hat{D}^\dagger(-\bar{\alpha})\hat{D}(\bar{\alpha})|p\rangle \\ &= \langle q|\hat{D}(2\bar{\alpha})|p\rangle = \mathcal{D}_{qp}(2\bar{\alpha}), \end{aligned}$$

$$\begin{aligned} \mathcal{A}_{2q,2p+1} &= \langle\phi_{2q}|\phi_{2p+1}\rangle = \langle q|\hat{D}^\dagger(\bar{\alpha})\hat{D}(-\bar{\alpha})|p\rangle \\ &= \langle q|\hat{D}(-2\bar{\alpha})|p\rangle = \mathcal{D}_{qp}(-2\bar{\alpha}), \end{aligned}$$

where $\mathcal{D}_{pq}(\alpha) = {}_c\langle p|\hat{D}(\alpha)|q\rangle_c$ are the elements of the representation $\mathcal{D}(\alpha)$ of the displacement operator $\hat{D}(\alpha)$ in the Bogoliubov mode's Fock basis. Noting that the displacement operator can be written as $\hat{D}(\alpha) = \exp(\alpha_c\hat{c}^\dagger - \alpha_c^*\hat{c})$, with $\alpha_c = \alpha \cosh \bar{r} - \alpha^* \sinh \bar{r}$, we have for $\alpha \in \mathbb{R}$ [26]

$$\mathcal{D}_{pq}(\alpha) = e^{-|\alpha_c|^2/2} \times \begin{cases} \sqrt{\frac{q!}{p!}} \alpha_c^{p-q} L_q^{(p-q)}(|\alpha_c|^2), & p \geq q \\ \sqrt{\frac{p!}{q!}} \alpha_c^{q-p} L_p^{(q-p)}(|\alpha_c|^2), & p < q \end{cases}, \quad (\text{B3})$$

where $L_n^{(a)}(x)$ are the generalized Laguerre polynomials.

Let us discuss now the representation of the Hamiltonian \hat{H} , which we assume to be written in anti-normal order, such that it is a sum of terms of the type $\hat{c}^m \hat{c}^{\dagger n}$ for different natural values of m and n . Note that, because the basis is not orthonormal, the representation of a product of operators is no longer the matrix product of their representations. Instead, we have to use the following expressions:

$$\begin{aligned} \langle\phi_{2q}|\hat{c}^m \hat{c}^{\dagger n}|\phi_{2p}\rangle &= \langle q|\hat{D}^\dagger(\bar{\alpha})\hat{c}^m \hat{D}(\bar{\alpha})\hat{D}^\dagger(\bar{\alpha})\hat{c}^{\dagger n} \hat{D}(\bar{\alpha})|p\rangle \\ &= \langle q|(\hat{c} + \bar{\alpha}_c)^m (\hat{c}^\dagger + \bar{\alpha}_c^*)^n |p\rangle \\ &= \sum_{r=0}^m \sum_{s=0}^n \binom{m}{r} \binom{n}{s} \bar{\alpha}_c^{m-r} (\bar{\alpha}_c^{n-s})^* \langle q|\hat{c}^r \hat{c}^{\dagger s}|p\rangle \\ &= \sum_{r=0}^m \sum_{s=0}^n \binom{m}{r} \binom{n}{s} \bar{\alpha}_c^{m-r} (\bar{\alpha}_c^{n-s})^* \\ &\quad \times \sqrt{\frac{(q+r)!(p+s)!}{q!p!}} \delta_{q+r,p+s}, \end{aligned} \quad (\text{B4})$$

with $\bar{\alpha}_c = \bar{\alpha}(\cosh \bar{r} - \sinh \bar{r})$, the same for $\langle\phi_{2q+1}|\hat{c}^m \hat{c}^{\dagger n}|\phi_{2p+1}\rangle$ changing $\bar{\alpha}$ by $-\bar{\alpha}$, and

$$\begin{aligned} \langle\phi_{2q+1}|\hat{c}^m \hat{c}^{\dagger n}|\phi_{2p}\rangle &= \langle q|\hat{D}^\dagger(-\bar{\alpha})\hat{c}^m \hat{c}^{\dagger n} \hat{D}(\bar{\alpha})|p\rangle \\ &= \langle q|(\hat{c} - \bar{\alpha}_c)^m \hat{D}(2\bar{\alpha}) (\hat{c}^\dagger + \bar{\alpha}_c^*)^n |p\rangle \\ &= \sum_{r=0}^m \sum_{s=0}^n \binom{m}{r} \binom{n}{s} (-\bar{\alpha}_c)^{m-r} (\bar{\alpha}_c^{n-s})^* \langle q|\hat{c}^r \hat{D}(2\bar{\alpha}) \hat{c}^{\dagger s}|p\rangle \\ &= \sum_{r=0}^m \sum_{s=0}^n \binom{m}{r} \binom{n}{s} (-\bar{\alpha}_c)^{m-r} (\bar{\alpha}_c^{n-s})^* \\ &\quad \times \sqrt{\frac{(q+r)!(p+s)!}{q!p!}} \mathcal{D}_{q+r,p+s}(2\bar{\alpha}), \end{aligned} \quad (\text{B5})$$

plus the same for $\langle\phi_{2q}|\hat{c}^m \hat{c}^{\dagger n}|\phi_{2p+1}\rangle$ changing $\bar{\alpha}$ by $-\bar{\alpha}$. Note that in the second equality, we have inserted the identity operator $\hat{D}(-\bar{\alpha})\hat{D}^\dagger(-\bar{\alpha})\hat{D}(\bar{\alpha})\hat{D}^\dagger(\bar{\alpha})$ in between \hat{c}^m and $\hat{c}^{\dagger n}$.

Appendix C: Equivalence between the thermodynamic and classical limits

A neat way of showing that quantum fluctuations are fixed to zero-point fluctuations in the thermodynamic limit $L \rightarrow \infty$ is by using the positive P phase-space representation of the state of the system [27, 28], which allows mapping the exact quantum dynamics into a set of stochastic differential equations. The positive P distribution can be seen as a generalization of the more familiar Glauber-Sudarshan P function $P(\alpha)$ [29]. The latter provides the coefficients required to expand a given density operator $\hat{\rho}$ as a linear combination of coherent-state projectors, that is, $\hat{\rho} = \int_{\mathbb{C}} \frac{d^2\alpha}{\pi} P(\alpha) |\alpha\rangle\langle\alpha|$. Quantum expectation values in normal order are then mapped to phase-space averages through $\langle\hat{a}^{\dagger m} \hat{a}^n\rangle = \int_{\mathbb{C}} \frac{d^2\alpha}{\pi} P(\alpha) \hat{a}^{*m} \hat{a}^n$.

Using the identities [27–29] $\hat{a}|\alpha\rangle = \alpha|\alpha\rangle$ and $\hat{a}^\dagger|\alpha\rangle\langle\alpha| = (\alpha^* + \partial_\alpha)|\alpha\rangle\langle\alpha|$, it is easy to rewrite the von Neumann equation for the evolution of the state, $\partial_t \hat{\rho} = -i[\hat{H}, \hat{\rho}]$, as the following partial differential equation for the distribution [29]:

$$\partial_t P = \left[-\partial_\alpha A(\alpha) + \frac{1}{2} \partial_\alpha^2 D(\alpha) \right] P + \text{c.c.}, \quad (\text{C1})$$

where

$$A = -i(1 + |\alpha|^2/L)\alpha + i\alpha^*, \quad (\text{C2a})$$

$$D = i(\varepsilon - \alpha^2/L). \quad (\text{C2b})$$

In terms of the real variables ($\text{Re}\{\alpha\}, \text{Im}\{\alpha\}$), Eq. (C1) has the form of a Fokker-Planck equation. However, the corresponding diffusion matrix is easily shown not to be positive semidefinite at some points of phase space. This is evidenced by the naive application of the equivalence [29] between the Fokker-Planck equation and the following set of stochastic Langevin equations: $\dot{\alpha} = A + \sqrt{D}\eta_1(t)$ and $\dot{\alpha}^* = A^* + \sqrt{D^*}\eta_2(t)$, where $\eta_j(t)$ are independent real Gaussian white noises. These are nonsensical equations, since α and α^* do not remain complex-conjugate under evolution. The positive P representation $P_+(\alpha, \alpha^+)$ is a generalization of the Glauber-Sudarshan function that allows finding a Fokker-Planck equation with a positive semidefinite diffusion matrix, but at the expense of working in a doubled phase space, since here α and α^+ are independent complex variables. It can be (non-uniquely) defined through [27, 28]

$$\hat{\rho} = \int_{\mathbb{C}^2} d^2\alpha d^2\alpha^+ P_+(\alpha, \alpha^+) \frac{|\alpha\rangle\langle\alpha^{+*}|}{\langle\alpha^{+*}|\alpha\rangle}, \quad (\text{C3})$$

for the representation of a state $\hat{\rho}$, where the states in the kernel are coherent. It can be shown that quantum expectation values are obtained as $\langle\hat{a}^{\dagger m} \hat{a}^n\rangle = \int_{\mathbb{C}^2} d^2\alpha d^2\alpha^+ P_+(\alpha, \alpha^+) \hat{a}^{+m} \hat{a}^n$. In addition, it is also shown that the corresponding stochastic Langevin equations can be obtained from the naive ones provided by the Glauber-Sudarshan representation, just replacing α^*

by α^+ [27, 28], that is,

$$\dot{\alpha} = -i \left(1 + \frac{\alpha^+\alpha}{L} \right) \alpha + i\alpha^+ + \sqrt{i \left(\varepsilon - \frac{\alpha^2}{L} \right)} \eta_1(t), \quad (\text{C4a})$$

$$\dot{\alpha}^+ = i \left(1 + \frac{\alpha^+\alpha}{L} \right) \alpha^+ - i\alpha + \sqrt{-i \left(\varepsilon - \frac{\alpha^{+2}}{L} \right)} \eta_2(t). \quad (\text{C4b})$$

Since now α and α^+ are independent complex variables, there are no issues with them not evolving as a complex-conjugate pair. It's important to note that these equations provide the exact quantum dynamics of observables, there are no approximations involved in their derivation. In addition, note that a coherent state $|\alpha_0\rangle$ can be represented by the distribution $P_+ = \delta^{(2)}(\alpha - \alpha_0) \delta^{(2)}(\alpha^+ - \alpha_0^*)$, meaning that whenever the solutions of (C4) do not fluctuate, the state of the system is given by a coherent state. This is exactly what happens in the $L \rightarrow \infty$ limit as we show next. In order to do this, let us normalize the variables as $\alpha = \sqrt{L}\beta$ and $\alpha^+ = \sqrt{L}\beta^+$, obtaining then

$$\dot{\beta} = -i \left(1 + \beta^+\beta \right) \beta + i\beta^+ + \sqrt{\frac{i}{L} \left(\varepsilon - \beta^2 \right)} \eta_1(t), \quad (\text{C5a})$$

$$\dot{\beta}^+ = i \left(1 + \beta^+\beta \right) \beta^+ - i\beta + \sqrt{-\frac{i}{L} \left(\varepsilon - \beta^{+2} \right)} \eta_2(t). \quad (\text{C5b})$$

This normalized equations clearly show that in the thermodynamic $L \rightarrow \infty$ limit, the noise term vanishes, since β and β^+ are finite. Hence, in this limit the deterministic part of the equations dominates, and the variables do not fluctuate when starting from non-fluctuating initial conditions. In other words, a coherent state remains coherent. This shows that, in our model, the thermodynamic and classical limits are not independent, but equivalent.

-
- [1] W. Greiner, *Thermodynamics and statistical mechanics* (Springer, New York, 1995).
 - [2] M. Heyl, *Reports on Progress in Physics* **81**, 054001 (2018).
 - [3] X.-G. Wen, *Rev. Mod. Phys.* **89**, 041004 (2017).
 - [4] M.-J. Hwang and M. B. Plenio, *Phys. Rev. Lett.* **117**, 123602 (2016).
 - [5] M.-J. Hwang, R. Puebla, and M. B. Plenio, *Phys. Rev. Lett.* **115**, 180404 (2015).
 - [6] S. Sachdev, *Quantum phase transitions* (Cambridge University Press, New York, 2011).
 - [7] L. P. Kadanoff, *Statistical physics* (World Scientific, Singapore, 2000).
 - [8] N. Goldenfeld, *Lectures on phase transitions and the renormalization group* (Perseus Books, Reading, 1992).
 - [9] M. Vojta, *Reports on Progress in Physics* **66**, 2069 (2003).
 - [10] V. Dobrosavljevic, *Conductor-insulator quantum phase transitions* (Oxford University Press, Oxford, 2012).
 - [11] A. Dutta, *Quantum phase transitions in transverse field spin models : from statistical physics to quantum information* (Cambridge University Press, Delhi, 2015).
 - [12] L. Carr, *Understanding quantum phase transitions* (CRC Press, Boca Raton, 2011).
 - [13] T. Vojta, “Computing quantum phase transitions,” (2007), [arXiv:0709.0964 \[cond-mat.stat-mech\]](https://arxiv.org/abs/0709.0964).
 - [14] D. Jaksch and P. Zoller, *Annals of Physics* **315**, 52 (2005).

- [15] I. Bloch, J. Dalibard, and W. Zwerger, [Rev. Mod. Phys.](#) **80**, 885 (2008).
- [16] I. Bloch, J. Dalibard, and S. Nascimbène, [Nat. Phys.](#) **8**, 267 (2012).
- [17] O. Dutta, M. Gajda, P. Hauke, M. Lewenstein, D.-S. Lühmann, B. A. Malomed, T. Sowiński, and J. Zakrzewski, [Rep. Prog. Phys.](#) **78**, 066001 (2015).
- [18] B. V. e. a. Roch N., Florens S., [Nature](#) **453**, 633 (2008).
- [19] I. G. Rau, S. Amasha, Y. Oreg, and D. Goldhaber-Gordon, (2013), [10.48550/ARXIV.1309.7737](#).
- [20] S. Suzuki, J.-i. Inoue, and B. K. Chakrabarti, *Quantum Ising phases and transitions in transverse Ising models* (Springer Verlag, Berlin, 1996).
- [21] L. Bakemeier, A. Alvermann, and H. Fehske, [Phys. Rev. A](#) **85**, 043821 (2012).
- [22] H. Lipkin, N. Meshkov, and A. Glick, [Nuclear Physics](#) **62**, 188 (1965).
- [23] P. Ribeiro, J. Vidal, and R. Mosseri, [Phys. Rev. E](#) **78**, 021106 (2008).
- [24] C. Navarrete-Benlloch, “Introduction to quantum optics,” (2022), [arXiv:2203.13206](#).
- [25] D. J. Griffiths and D. F. Schroeter, *Introduction to quantum mechanics* (Cambridge University Press, New York, 2018).
- [26] K. E. Cahill and R. J. Glauber, [Phys. Rev.](#) **177**, 1857 (1969).
- [27] P. D. Drummond and C. W. Gardiner, [Journal of Physics A: Mathematical and General](#) **13**, 2353 (1980).
- [28] H. J. Carmichael, *Statistical methods in quantum optics 2: Non-classical fields* (Springer Verlag, Berlin, 2008).
- [29] H. J. Carmichael, *Statistical methods in quantum optics 1: Master equations and Fokker-Planck equations* (Springer Verlag, Berlin, 1999).